

Probing the electroweak $4b + \ell + \cancel{E}_T$ final state in type I 2HDM at the LHC

Prasenjit Sanyal and Daohan Wang

Department of Physics, Konkuk University, Seoul 05029, Republic of Korea

E-mail: prasenjit.sanyal01@gmail.com, wdh9508@gmail.com

ABSTRACT: Most of the experimental searches of the non-Standard Model Higgs boson(s) at the LHC rely on the QCD induced production modes. However, in some beyond Standard Model frameworks, the additional Higgs bosons can have fermiophobic behaviour. The type I two Higgs doublet model considered here is a perfect example where all the additional Higgs bosons exhibit fermiophobic nature over a large region of parameter space. Thus the electroweak productions of these new Higgs bosons are more dominant over the QCD induced processes. In scenarios with light pseudoscalar (A) which is bound to decay dominantly to $b\bar{b}$, even being fermiophobic, the $4b + W$ state via $pp \rightarrow H^\pm A \rightarrow (AW)A \rightarrow 4b + W$ and followed by the leptonic decay of W boson can surpass the QCD initiated $4b$ final state. However, the signal gets overshadowed by large $t\bar{t}$ +jets background and hence constructing a suitable discriminator based on the signal hypothesis and signal topology is necessary. We devised a χ^2 variable as the most suitable signal-background discriminator to reduce the background by a sizable amount and showed the discovery reach ($> 3\sigma$) of the electroweak initiated $4b + \ell + \cancel{E}_T$ final state at the LHC.

Contents

| | | |
|----------|--|-----------|
| 1 | Introduction | 1 |
| 2 | Type I 2HDM review | 3 |
| 3 | Electroweak $4b + \ell + \cancel{E}_T$ state | 5 |
| 3.1 | χ^2 Method | 8 |
| 3.2 | Signal-background analysis | 11 |
| 4 | Conclusions | 15 |

1 Introduction

The Standard Model (SM) is currently the most extensively tested model for particle physics as all the collider experiments are in perfect agreement with it. The discovery of Higgs boson [1–4] gives SM the stature of the only acceptable theory in the energy scale of the present day colliders. However, despite its success, SM is believed neither a complete, nor a perfect theory because of several drawbacks. SM cannot explain the matter-antimatter asymmetry, neutrino oscillation, existence of dark matter, mass hierarchy within elementary particles and does not include gravity. Also there is no fundamental reason in support of one scalar particle, i.e. the Higgs sector in the SM is assumed to be minimal under the electroweak gauge symmetry. The observation of any other scalar particle, whether neutral or charged, will provide a strong indication of the non-minimal framework for the Electroweak Symmetry Breaking (EWSB).

The two Higgs doublet model (2HDM) [5–8] is the simplest extension of SM which accommodates a second Higgs doublet with the same quantum numbers as the first one. The most general 2HDM where both the Higgs doublets couple to the fermions suffer from Flavor Changing Neutral Currents (FCNC) which contradicts with the experiments. To prevent the FCNC, a \mathbb{Z}_2 symmetry is imposed [9, 10] which restricts the Yukawa sector in to four possible types, viz type I, type II, type X and type Y. Each type of 2HDM has its own characteristics, which makes 2HDM a phenomenologically very rich extension of SM. After the EWSB, the scalar sector in the CP conserving framework of 2HDM consists of two CP even scalars h , H , a CP odd scalar (pseudoscalar) A and a pair of charged Higgs H^\pm . We follow the standard mass hierarchy where the observed 125 GeV Higgs boson, identified by h , is the lightest CP even Higgs boson.

The conventional search strategies to look for neutral single Higgs or multi-Higgs states at the Large Hadron Collider (LHC) involves the QCD induced processes like gluon fusion process or the $b\bar{b}$ -annihilation [11–23], where the b -quarks are themselves produced from a (double) gluon splitting. Even for single production of the charged Higgs, the usual search

for light charged Higgs is given by the top quark pair production cross section times the branching ratio of top into charged Higgs and the top-bottom associated production for heavy charged Higgs [24–27]. Thus all these channels are intrinsically gg -induced. However, the QCD induced processes can be subdominant in some beyond SM (BSM) frameworks where the fermionic couplings to the BSM particles are suppressed. The type I 2HDM fits this criteria as all the BSM Higgs bosons show fermiophobic behaviour [28–38]. In such situation the production of the BSM Higgses through EW processes get more importance than the QCD induced processes [31, 35, 36]. Similarly, the bosonic decays of the BSM Higgses can overcome the fermionic decay modes if kinematically allowed [30, 32, 36]. In type I 2HDM, the EW production of a light A in association with H^\pm and followed by H^\pm decay to AW can give the AAW mode. Since the AAW mode involves $q\bar{q}'$ -induced production where q represents valence quark (u, d), the AAW mode has no QCD production counterpart. For the situation of light A , the decays of A are restricted only to the fermions and the branching ratio of $A \rightarrow b\bar{b}$ is dominant¹. This gives rise to the $4b + W$ mode. Considering the leptonic decay of the W boson, we can have $4b + \ell + \cancel{E}_T$ final state, which as mentioned before is the signature state characteristic of the EW processes and can dominate over the QCD induced $4b$ state for a large parameter space. The $4b + \ell + \cancel{E}_T$ final state also have subdominant contributions from other EW processes e.g. through the production channels $pp \rightarrow H^\pm H/H^+H^-$ and thereafter the decay chains $H^\pm \rightarrow AW$ and $H \rightarrow AA/AZ$. Contribution to $4b + W$ through $pp \rightarrow H^\pm h$ with $H^\pm \rightarrow hW$ and $h \rightarrow b\bar{b}$ are highly suppressed due to the alignment limit and hence not considered in our work. Since we are restricted to the standard mass hierarchy with light A , only $A \rightarrow b\bar{b}$ decay can give large cross section for the final state of our interest. Situation with inverted mass hierarchy with 125 GeV Higgs as the heavier CP even Higgs, identified by H , the light CP even Higgs h can decay dominantly to $b\bar{b}$ and we can obtain the $4b + W$ state via the hhW production mode [35, 39, 40]. Interestingly, in the inverted scenario, fermiophobic limit of h gives large $h \rightarrow \gamma\gamma/WW^*$ decay modes [33, 38, 41] compared to the $b\bar{b}$ mode. Whereas, slight deviation from the fermiophobic limit of h makes the decay into $b\bar{b}$ and $\gamma\gamma$ modes comparable, leading to $2b2\gamma + W$ final state [42] which serves as a complementary channel to the $4b + W$ state.

At the LHC the dominant SM background for the proposed final state, the $t\bar{t}$ +jets background, is significantly higher than the EW $4b + \ell + \cancel{E}_T$ final state. Hence we require strong selection cuts which can kill the background. In this work we construct a χ^2 variable, which is based on the signal topology and the signal hypothesis (masses of A and H^\pm). The χ^2 can be used to discriminate the signal and the background and therefore highly effective in reducing the background significantly without affecting much the signal. The most appropriate use for χ^2 would be for the mass reconstruction of the BSM Higgs bosons [33, 43], however we can only reconstruct the masses of A and H^\pm via $4b + \ell + \cancel{E}_T$ final state. To probe the full Higgs spectrum, the EW induced inclusive $4b + X$ final state (where X implies any additional jets even b -jets and /or leptons) is more suitable. In our recent study [44], we showed that the EW initiated $4b + X$ can provide simultaneous reconstruction of

¹We also have $A \rightarrow gg$ decay mode via top/bottom loop, but very suppressed

all the BSM Higgs boson masses. Hence, instead of using χ^2 for the reconstruction of the masses of A and H^\pm , we use χ^2 as a selection criteria to discriminate the signal from the background. Along with the χ^2 we use other selection cuts like the asymmetry cut and di-jet η separation cuts to obtain the discovery significance of the signal at the 13 TeV LHC with 3000 fb^{-1} luminosity.

The article is organized as follows. In Sec.[2] we give an overview of type I 2HDM and discuss the fermionic and gauge couplings of the additional Higgs bosons to show the fermiophobic natures as well as the Higgs trilinear couplings. In Sec.[3], we discuss the signal topology of the AAW mode, it's production cross section at the LHC and the dominant $t\bar{t}$ +jets background. We show the theoretical and experimental constraints on the model parameters, the formalism of χ^2 method and the signal-background analysis. Finally we conclude in Sec.[4].

2 Type I 2HDM review

The most general scalar potential for the 2HDM is

$$\begin{aligned} \mathcal{V}(\Phi_1, \Phi_2) = & m_{11}^2 \Phi_1^\dagger \Phi_1 + m_{22}^2 \Phi_2^\dagger \Phi_2 - [m_{12}^2 \Phi_1^\dagger \Phi_2 + h.c.] + \frac{1}{2} \lambda_1 (\Phi_1^\dagger \Phi_1)^2 \\ & + \frac{1}{2} \lambda_2 (\Phi_2^\dagger \Phi_2)^2 + \lambda_3 (\Phi_1^\dagger \Phi_1) (\Phi_2^\dagger \Phi_2) + \lambda_4 (\Phi_1^\dagger \Phi_2) (\Phi_2^\dagger \Phi_1) \\ & + \left\{ \frac{\lambda_5}{2} (\Phi_1^\dagger \Phi_2)^2 + [\lambda_6 (\Phi_1^\dagger \Phi_1) + \lambda_7 (\Phi_2^\dagger \Phi_2)] (\Phi_1^\dagger \Phi_2) + h.c. \right\} \end{aligned} \quad (2.1)$$

where $\Phi_{1,2}$ are the two Higgs doublets with hypercharge $Y = 1/2$ and the parameters m_{11}^2 , m_{22}^2 and $\lambda_{1,2,3,4}$ are real for the scalar potential to be real. The other parameters m_{12}^2 and $\lambda_{5,6,7}$ in general can be complex. To avoid the tree level FCNC, a \mathbb{Z}_2 symmetry is imposed under which $\Phi_1 \rightarrow \Phi_1$ and $\Phi_2 \rightarrow -\Phi_2$ which implies $\lambda_{6,7} = 0$. However, the \mathbb{Z}_2 symmetry is softly broken by the dimensionful parameter $m_{12}^2 \neq 0$. Assuming CP invariant framework, m_{12}^2 and λ_5 are considered real. The two Higgs doublets are parameterized as

$$\Phi_i = \begin{pmatrix} H_i^+ \\ \frac{v_i + h_i + iA_i}{\sqrt{2}} \end{pmatrix}, \quad i = 1, 2. \quad (2.2)$$

After EWSB, the scalar spectrum consists of two CP even scalars h and H , one CP odd pseudoscalar A and a pair of charged Higgs H^\pm . The physical mass eigenstates are related to the gauge eigenstates by the following equations

$$\begin{pmatrix} H \\ h \end{pmatrix} = \begin{pmatrix} c_\alpha & s_\alpha \\ -s_\alpha & c_\alpha \end{pmatrix} \begin{pmatrix} h_1 \\ h_2 \end{pmatrix}, \quad A = -s_\beta A_1 + c_\beta A_2, \quad H^\pm = -s_\beta H_1^\pm + c_\beta H_2^\pm \quad (2.3)$$

where $v_{1,2}$ are the vacuum expectation values (VEVs) of the two Higgs doublets such that $v = \sqrt{v_1^2 + v_2^2} = 246 \text{ GeV}$ and we define the parameter $t_\beta = v_2/v_1$. We use the abbreviations, $s_\alpha(c_\alpha) = \sin \alpha(\cos \alpha)$, $s_\beta(c_\beta) = \sin \beta(\cos \beta)$, $t_\beta = \tan \beta$, etc. We identify the physical state h as the SM-like observed Higgs boson of mass 125 GeV as all the Higgs signal strength measurements [45–57] are consistent with SM. Throughout the paper we collectively call H , A and H^\pm as the beyond SM (BSM) Higgs bosons.

| | | | | | | | | | |
|--------|--------------------|--------------------|--------------------|--------------------|--------------------|--------------------|-------------|--------------|--------------|
| 2HDM | ξ_h^u | ξ_h^d | ξ_h^ℓ | ξ_H^u | ξ_H^d | ξ_H^ℓ | ξ_A^u | ξ_A^d | ξ_A^ℓ |
| type-I | c_α/s_β | c_α/s_β | c_α/s_β | s_α/s_β | s_α/s_β | s_α/s_β | $1/t_\beta$ | $-1/t_\beta$ | $-1/t_\beta$ |

Table 1. The Yukawa coupling modifiers in type I 2HDM

In type I 2HDM the fermion fields transform odd under the \mathbb{Z}_2 symmetry and therefore couple only to the second Higgs doublet Φ_2 . Hence the quarks and charged leptons get their masses from the VEV of Φ_2 . The Yukawa Lagrangian in type I 2HDM can be written as

$$\mathcal{L}_Y^I = -\bar{Q}_L Y_u \tilde{\Phi}_2 u_R - \bar{Q}_L Y_d \tilde{\Phi}_2 d_R - \bar{L}_L Y_\ell \Phi_2 \ell_R + h.c. \quad (2.4)$$

where $\tilde{\Phi}_2 = i\tau_2 \Phi_2^*$. After the EWSB, the Yukawa Lagrangian in terms of the mass eigenstates is

$$\begin{aligned} \mathcal{L}_Y^I = & - \sum_{f=u,d,\ell} \frac{m_f}{v} \left(\xi_h^f \bar{f} f h + \xi_H^f \bar{f} f H - i \xi_A^f \bar{f} f \gamma_5 A \right) \\ & - \left\{ \frac{\sqrt{2} V_{ud}}{v} \bar{u} \left(\xi_A^u m_u P_L + \xi_A^d m_d P_R \right) d H^+ + \frac{\sqrt{2} m_\ell}{v} \xi_A^\ell \bar{\nu}_L \ell_R H^+ + h.c. \right\} \end{aligned} \quad (2.5)$$

where V is the CKM matrix and $P_{L,R} = \frac{1}{2}(1 \mp \gamma_5)$ are the chirality projection operators. The Yukawa coupling modifiers ξ^f are given in Table. [1]. The gauge boson couplings to the scalar fields in 2HDM are independent of the Yukawa types. The couplings of the neutral scalars to a pair of gauge bosons are

$$g_{hVV} = s_{\beta-\alpha} g_{hVV}^{SM}, \quad g_{HV V} = c_{\beta-\alpha} g_{hVV}^{SM}, \quad g_{AVV} = 0 \quad (2.6)$$

where $V = W^\pm, Z$. The Z boson couplings to the neutral scalars are

$$g_{hAZ_\mu} = \frac{g}{2c_{\theta_W}} c_{\beta-\alpha} (p_h - p_A)_\mu, \quad g_{HAZ_\mu} = -\frac{g}{2c_{\theta_W}} s_{\beta-\alpha} (p_H - p_A)_\mu \quad (2.7)$$

where p_μ represent the incoming four momenta of the Higgs bosons, g denotes the $SU(2)_L$ gauge coupling and θ_W is the Weinberg angle. Similarly the W boson couplings to the charged Higgs are

$$\begin{aligned} g_{H^\mp W^\pm h} &= \mp \frac{ig}{2} c_{\beta-\alpha} (p_h - p_{H^\mp})_\mu, \\ g_{H^\mp W^\pm H} &= \pm \frac{ig}{2} s_{\beta-\alpha} (p_H - p_{H^\mp})_\mu, \\ g_{H^\mp W^\pm A} &= \frac{g}{2} (p_A - p_{H^\mp})_\mu \end{aligned} \quad (2.8)$$

with incoming four momenta of the neutral and charged Higgs. From the Table. [1], we can see that the fermionic couplings of H^\pm and A are suppressed at large t_β and thus their behaviour is fermiophobic. Another important factor is the alignment limit $s_{\beta-\alpha} \rightarrow 1$ [58, 59] which is mostly favored by the experimental constraints so that all the couplings of

h approach to that of the SM. The alignment limit together with large t_β also make the H fermiophobic. This can be seen from the Yukawa coupling modifier of H

$$\xi_H^f = \frac{s_\alpha}{s_\beta} = c_{\beta-\alpha} - \frac{s_{\beta-\alpha}}{t_\beta}. \quad (2.9)$$

In the limit of $s_{\beta-\alpha} \rightarrow 1$ and $t_\beta \gg 1$, ξ_H^f approaches to zero. The fermiophobic behaviour of the BSM Higgs bosons is the most striking characteristics of type I 2HDM.

For A lighter than half of the mass of the SM Higgs, strong constraint comes from the non-SM $h \rightarrow AA$ decay. The Higgs trilinear coupling which involves in this decay process is given by

$$\lambda_{hAA} = \frac{1}{4v^2 s_\beta c_\beta} \left\{ (4M^2 - 2m_A^2 - 3m_h^2)c_{\alpha+\beta} + (2m_A^2 - m_h^2)c_{\alpha-3\beta} \right\} \quad (2.10)$$

and the decay width is given as

$$\Gamma(h \rightarrow AA) = \frac{\lambda_{hAA}^2 v^2}{32\pi m_h} \sqrt{1 - \frac{4m_A^2}{m_h^2}} \quad (2.11)$$

where $M^2 = m_{12}^2/s_\beta c_\beta$. This trilinear coupling λ_{hAA} is non vanishing even at the alignment limit $s_{\beta-\alpha} \rightarrow 1$.

$$\lambda_{hAA} = \frac{1}{v^2} (2M^2 - 2m_A^2 - m_h^2), \quad \forall s_{\beta-\alpha} \rightarrow 1. \quad (2.12)$$

Other trilinear couplings related to the decays of H are λ_{Hhh} and λ_{HAA} , which are given as

$$\lambda_{Hhh} = \frac{1}{2v^2 s_\beta c_\beta} c_{\beta-\alpha} \left\{ (3M^2 - 2m_h^2 - m_H^2)s_{2\alpha} - M^2 s_{2\beta} \right\}, \quad (2.13)$$

$$\lambda_{HAA} = \frac{1}{4v^2 s_\beta c_\beta} \left\{ (4M^2 - 2m_A^2 - 3m_H^2)s_{\alpha+\beta} - (m_H^2 - 2m_A^2)s_{\alpha-3\beta} \right\} \quad (2.14)$$

and in the alignment limit, λ_{Hhh} vanishes and λ_{HAA} reduces to

$$\lambda_{HAA} = \frac{2}{v^2 t_{2\beta}} (m_H^2 - M^2). \quad (2.15)$$

For light A , the mass splitting between H^\pm and H is highly restricted by the electroweak precision observables, as we will see later, we do not discuss the HH^+H^- coupling. Thus the fermiophobic nature restricts the decay of H only to the AA and AZ modes in the alignment limit.

3 Electroweak $4b + \ell + \cancel{E}_T$ state

In type I 2HDM, the QCD production processes of BSM Higgs bosons are usually suppressed compared to the EW processes due to the fermiophobic behaviour. Not only that, the

bosonic decays (both on-shell and off-shell) of $H^\pm \rightarrow AW^{(*)}$ and $H \rightarrow AA/AZ^{(*)}$ can be the dominant decay modes. Since in our paper we are restricted to light A , the branching ratio of $A \rightarrow b\bar{b}$ is dominant even though being fermiophobic. Hence, the most promising channel to search for light A is

$$AAW : pp \rightarrow H^\pm A \rightarrow (AW)A \rightarrow 4b + W \quad (3.1)$$

where the signal topology suggests that the prompt A should have higher p_T compared to the A from the decay of H^\pm [44]. To reduce the QCD multijet background we consider the leptonic decay of W boson. The $4b + \ell + \cancel{E}_T$ would be the final state we are looking for at the LHC. The cross section of the signal at the parton level is

$$\sigma_{AAW} = \sigma(pp \rightarrow H^\pm A)BR(H^\pm \rightarrow AW)BR(A \rightarrow b\bar{b})^2BR(W \rightarrow l\nu) \quad (3.2)$$

where in the lepton we also include τ . We use a uniform Next-to-Next-to-Leading Order (NNLO) k -factor of 1.35 [34].

The dominant background will be the top quark pair production where top quarks decay dominantly to bW mode and the semileptonic and leptonic (including τ) decays of W boson would give at least one lepton. The extra b -jets can come from the additional hard jets and from the hadronic decays of W boson faking as b -jets. Also for our analysis we generate $t\bar{t}$ background matched up to one parton using the MLM scheme [60, 61]. The cross section for the $t\bar{t}$ +jets background into fully leptonic and semileptonic states is 458 pb as calculated with Top++ [62]. Furthermore, in the case of other backgrounds such as Wjj and Zjj , the probability of a QCD jet being misidentified as a b -jet is only around 1% [63]. Hence by mimicing four b -jets, the Wjj and Zjj backgrounds can be effectively suppressed and rendered subdominant. Thus for our analysis we consider $t\bar{t}$ +jets as the only background. The cross section is given by

$$\sigma_{BG} = \sigma(pp \rightarrow t\bar{t} + jets)BR(t \rightarrow bW)^2BR(W \rightarrow l\nu)[2 - BR(W \rightarrow l\nu)]. \quad (3.3)$$

Before going to the phenomenological study of our signal, we scan the parameter space with two fixed masses of A viz, 50 GeV and 70 GeV. We restrict our study in the scenario of standard mass hierarchy where we assign the lightest CP even Higgs h as the observed 125 GeV Higgs and H as the heavier CP -even Higgs. The model parameters are scanned within the range

$$\begin{aligned} m_{H^\pm} &: [80 - 350] \text{ GeV}, & m_H &: [140 - 350] \text{ GeV}, & t_\beta &: [1 - 60] \\ s_{\beta-\alpha} &: [0.9 - 1.0], & m_{12}^2 &: [0 - 350^2] \text{ GeV}^2. \end{aligned} \quad (3.4)$$

We randomly generate sample points within the scanning range and apply the theoretical and experimental constraints to obtain the allowed parameter space as listed below. It is worth noting that recent advances in machine learning driven sampling methods [64] can greatly reduce the computational time of such scans.

1. **Theoretical Constraints:** The quartic couplings of the scalar potential should be $|\lambda_i| < 4\pi$ [65] to satisfy the perturbativity condition. The vacuum stability requires

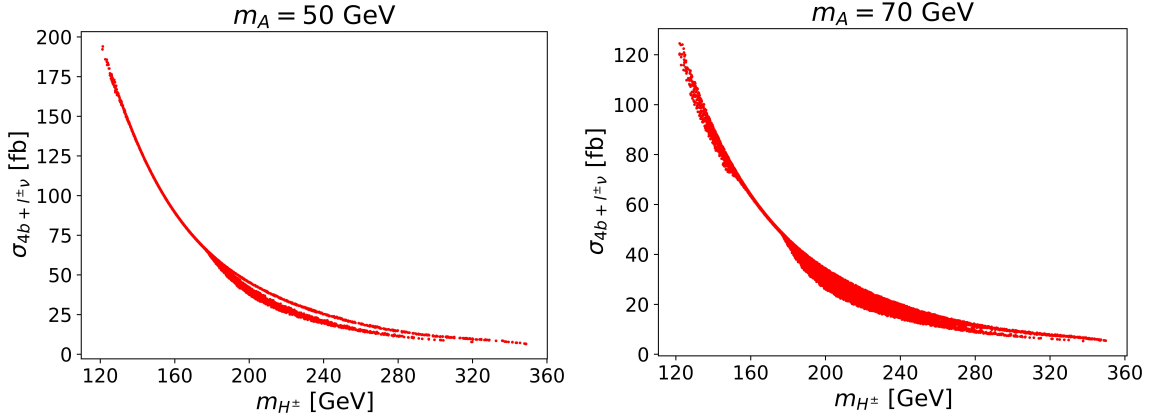


Figure 1. Signal cross sections for the AAW mode with $A \rightarrow b\bar{b}$ and $W \rightarrow l\nu$. Left: $m_A = 50 \text{ GeV}$ and Right: $m_A = 70 \text{ GeV}$.

the potential to be bounded from below and this gives us the constraints [66]

$$\lambda_{1,2} > 0, \quad \lambda_3 > -\sqrt{\lambda_1\lambda_2}, \quad \lambda_3 + \lambda_4 - |\lambda_5| > -\sqrt{\lambda_1\lambda_2}. \quad (3.5)$$

The tree-level unitarity of the Higgs boson and gauge boson scatterings at high energy as discussed in [67, 68] are also considered. The theoretical constraints are computed using the public code 2HDMC-1.8.0 [69].

2. **Electroweak Precision Observables:** The measurement of the oblique parameters, S , T and U restricts the mass splitting between the BSM Higgs bosons in the 2HDM, particularly between the charged Higgs H^\pm and the other BSM neutral Higgs bosons (H, A). The current best fit results [70] at 95% C.L. are $S = -0.01 \pm 0.07$ and $T = 0.04 \pm 0.06$ with the correlation $\rho_{ST} = 0.92$ for $U = 0$. For the scenario of light A , the mass splitting between H^\pm and H gets restricted. We use 2HDMC for the computation of the oblique parameters based on the Refs.[71, 72].
3. **Flavor Physics Constraints:** The B -physics observables are calculated using the code SuperIso-v4.1 [73]. The limits on $B \rightarrow X_s\gamma$ transition rate [74, 75] excludes $t_\beta \lesssim 2$ at 95% C.L. in the $m_{H^\pm} - t_\beta$ plane [75, 76] for type I 2HDM, thus reflecting the fermiophobic behaviour of H^\pm with respect to t_β .
4. **Collider Constraints:** The exclusion limits for the direct Higgs boson searches at LEP, Tevatron and LHC at 95% C.L. are imposed by using the public code HiggsBounds-v5.10.2 [77]. Along with the direct searches, we also check the consistency of the Higgs precision measurements using the code HiggsSignals-v2.6.2 [78]. We find the allowed parameter points at 95% C.L. with respect to the best fit point in two dimensional parameter spaces, which corresponds to $\Delta\chi_{\text{HS}}^2 = \chi_{\text{HS}}^2 - \chi_{\text{HS,min}}^2 \lesssim 6$. The $\chi_{\text{HS,min}}^2$ for the best fit points of $m_A = 50 \text{ GeV}$ and 70 GeV cases are approximately 92 and 90 respectively.

| Signals | m_A [GeV] | m_{H^\pm} [GeV] | m_H [GeV] | $s_{\beta-\alpha}$ | m_{12}^2 [GeV ²] | t_β |
|---------|-------------|-------------------|-------------|--------------------|--------------------------------|-----------|
| BP1 | 50 | 142.811 | 141.438 | 0.95771 | 1209.72 | 15.9983 |
| BP2 | 50 | 184.916 | 161.629 | 0.95998 | 2333.38 | 10.7302 |
| BP3 | 50 | 225.747 | 208.539 | 0.95998 | 4724.73 | 8.4401 |
| BP4 | 70 | 152.41 | 159.024 | 0.98344 | 3123.09 | 6.05755 |
| BP5 | 70 | 190.812 | 177.972 | 0.98955 | 3651.57 | 8.09766 |
| BP6 | 70 | 236.081 | 219.12 | 0.96523 | 6073.61 | 7.04902 |

Table 2. Benchmark points with $m_A = 50$ and 70 GeV.

After imposing all the constraints we obtain the allowed parameter space, for which we compute the parton level cross sections for the signal [3.1], considering the leptonic decay of W boson as shown in Fig.[1]. For $m_A = 50$ GeV, $h \rightarrow AA$ decay is allowed. The constraints from the SM Higgs exotic decay includes $h \rightarrow AA \rightarrow bbbb$ ATLAS [79], $h \rightarrow AA \rightarrow bb\tau\tau$ CMS [80], $h \rightarrow AA \rightarrow bb\mu\mu$ ATLAS [81] CMS [82, 83], $h \rightarrow AA \rightarrow \tau\tau\tau\tau$ CMS [82], $h \rightarrow AA \rightarrow \tau\tau\mu\mu$ CMS [82, 84]. Along with these, strong constraints also come from the precisely measured Higgs decay width [85–88], thus restricting the Higgs trilinear coupling, $|\lambda_{hAA}| \lesssim 0.013$. To study the discovery prospects of the signal at the LHC, we proceed our analysis with some benchmark points (BPs) as given in Table. [2].

3.1 χ^2 Method

We see from Fig.[1], the cross sections of the signal is only of the order of 100 fb, however, the $t\bar{t}$ +jets background cross section (458 pb) is significantly higher than the signal. Thus simple cut based analysis based on n_b , p_T , ΔR , E_T variables are not sufficient to probe any excess of the signal over the background. Thus we need to construct suitable variable or discriminator based on the signal topology and signal hypothesis e.g. masses of the new physics which are m_{H^\pm} and m_A in our case. In this work we construct a χ^2 which is given by

$$\chi^2 = \left(\frac{m_{bb} - m_A}{\sigma_{m_A}} \right)^2 + \left(\frac{m_{bb\nu} - m_{H^\pm}}{\sigma_{m_{H^\pm}}} \right)^2. \quad (3.6)$$

We explain the χ^2 method in the following way:

1. **b -jet pairing algorithm:** The AAW signal would give at least four resolved b -jets and one lepton final state. Two b -jet pairs are constructed out of the four leading b -jets. There are three possible combinations to make b -jet pairs. We use subscripts 1 and 2 to refer the b -jet pairs. A jet pairing algorithm is used to choose one of the three possible combinations. We label the b -jets with the subscript a, b, c and d and the three combinations would be (1,2; 3,4), (1,3; 2,4) and (1,4; 2,3). The pairing algorithm considers the combination which minimises [89, 90]

$$\Delta R = |(\Delta R_1 - 0.8)| + |(\Delta R_2 - 0.8)| \quad (3.7)$$

where ΔR_1 and ΔR_2 for a particular combination are given by

$$\begin{aligned}\Delta R_1 &= \sqrt{(\eta_a - \eta_b)^2 + (\phi_a - \phi_b)^2}, \\ \Delta R_2 &= \sqrt{(\eta_c - \eta_d)^2 + (\phi_c - \phi_d)^2}.\end{aligned}\tag{3.8}$$

The pairing algorithm is motivated by the idea that the b -jets from the pseudoscalars would be closer together compared to the uncorrelated b -jets. The offset of 0.8 is used to reduce the pairings where the b -jets overlap in the $\eta - \phi$ space.

2. **Calculating $p_{z\nu}$ of neutrino:** In the AAW signal, we consider the leptonic decay of W boson. However, since there is no reconstructed object at the detector that corresponds to the neutrino, only the transverse component of the momentum can be inferred from the conservation of momentum: $\vec{p}_{T\nu} = -\sum_i \vec{p}_{T_i}$ (i includes the observed particles).

The z -component can be computed using the on-shell condition

$$m_W^2 = (E_\ell + E_\nu)^2 - (\vec{p}_\ell + \vec{p}_\nu)^2.\tag{3.9}$$

Rewriting this in terms of the x, y, z components of the neutrino momentum, we get a quadratic equation

$$Ap_{z\nu}^2 + Bp_{z\nu} + C = 0\tag{3.10}$$

where the coefficients are

$$\begin{aligned}A &= 4(E_\ell^2 - p_{z\ell}^2), \\ B &= -4ap_{z\ell}, \\ C &= 4E_\ell^2(p_{x\nu}^2 + p_{y\nu}^2) - a^2\end{aligned}\tag{3.11}$$

and $a = m_W^2 - m_\ell^2 + 2p_{x\ell}p_{x\nu} + 2p_{y\ell}p_{y\nu}$. Solving Eq.[3.10] we get

$$p_{z\nu} = \frac{-B \pm \sqrt{B^2 - 4AC}}{2A}\tag{3.12}$$

and in the case of imaginary root, the real component has to be considered. The estimation of the z -component of the neutrino momentum is possible when the missing transverse momentum corresponds to one neutrino. If the process consists of multiple neutrinos the above method does not hold true. Thus the method of obtaining $p_{z\nu}$ is appropriate strictly for $W \rightarrow e\nu_e$ and $W \rightarrow \mu\nu_\mu$ but not for $W \rightarrow \tau\nu_\tau \rightarrow e2\nu_\tau\nu_e$ and $W \rightarrow \tau\nu_\tau \rightarrow \mu2\nu_\tau\nu_\mu$. The direct production of e/μ via W boson decay amounts to 22% of the total W boson decay width. Whereas, the indirect production of e/μ via $W \rightarrow \tau\nu_\tau$ decay is only 4% of the W boson decay and therefore contributes insignificantly. Hence, we consider e/μ production via $W \rightarrow \tau\nu_\tau$ in conjunction with $W \rightarrow e\nu_e$ and $W \rightarrow \mu\nu_\mu$ to implement the above procedure.

3. **Mass resolutions:** The mass resolution refers to the expected uncertainty in the measurement of the masses of the BSM particles at the detector. The signal AAW

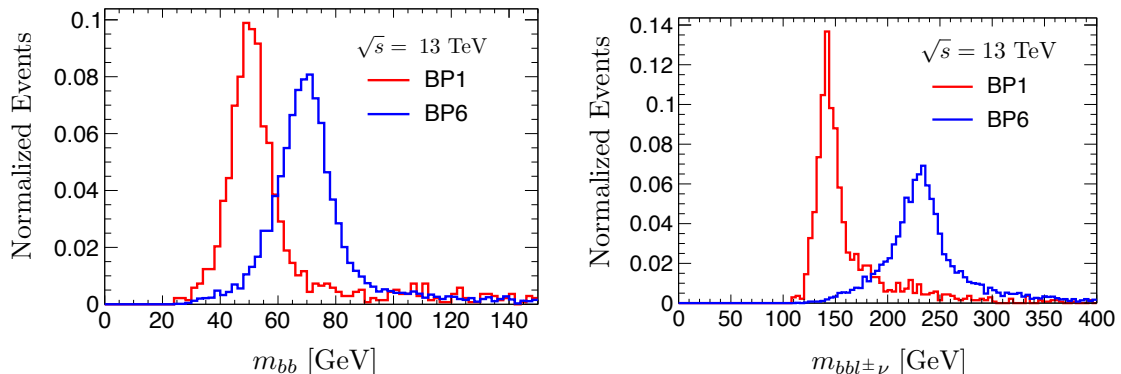


Figure 2. m_{bb} and $m_{bbl\nu}$ distributions normalized to one event for the BP1 and BP6. The FWHM gives the mass resolutions, σ_{m_A} and $\sigma_{m_{H^\pm}}$ respectively.

| Signals | m_A [GeV] | m_{H^\pm} [GeV] | σ_{m_A} [GeV] | $\sigma_{m_{H^\pm}}$ [GeV] |
|---------|-------------|-------------------|----------------------|----------------------------|
| BP1 | 50 | 142.811 | 13.97 | 19.92 |
| BP2 | 50 | 184.916 | 12.13 | 35.81 |
| BP3 | 50 | 225.747 | 12.14 | 36.15 |
| BP4 | 70 | 152.41 | 17.92 | 28.19 |
| BP5 | 70 | 190.812 | 18.00 | 28.00 |
| BP6 | 70 | 236.081 | 17.92 | 40.23 |

Table 3. Mass resolutions of A and H^\pm for the selected BPs.

has two pseudoscalars, one of the pseudoscalar comes from the decay of H^\pm and the other is the prompt pseudoscalar. To a good approximation we can assume that the leading b -jet comes from the prompt A . We can reconstruct the mass of A from the invariant mass distribution of the b -jet pair which contains the leading b -jet. The other b -jet pair together with the lepton and the neutrino reconstructs the mass of H^\pm . However, since the neutrino cannot be observed at the detector, we cannot estimate the 4-momentum of the neutrino². Hence the neutrino used for the truth reconstruction of H^\pm is the generator level neutrino [43]. The mass resolutions σ_{m_A} and $\sigma_{m_{H^\pm}}$ are estimated by obtaining the full width at half maximum (FWHM) of the invariant mass distributions of m_{bb} and $m_{bbl\nu}$. Fig.[2] gives the mass resolutions of both A and H^\pm for BP1 and BP6 and Table. [3] gives the mass resolutions of the selected BPs³. These mass resolutions are used as inputs to χ^2 in Eq.[3.6].

²The above method of $p_{z\nu}$ gives two possible solutions instead of exact solution required to reconstruct the 4-momentum.

³The mass resolutions obtained from the widths of the invariant mass distributions depend on the detector sensitivity, which in our case is consistent when we compare with the mass resolutions of W boson and top quark mentioned in Ref.[43].

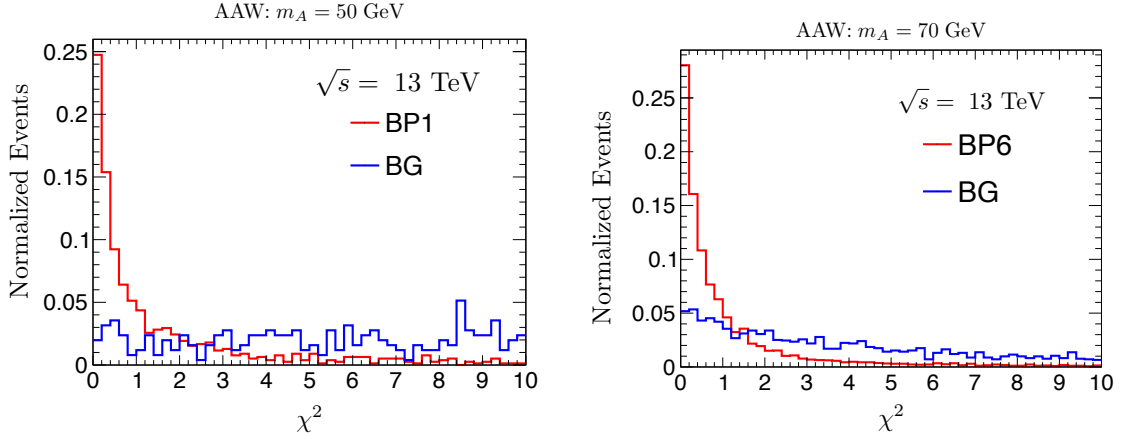


Figure 3. χ^2 distributions normalized to one event for the signal (via AAW mode) and background.

4. χ^2 **per event:** The χ^2 based on the signal hypothesis will be used to obtain an excess of $4b + \ell + \cancel{E}_T$ over the background. In each event (signal and background), we compute the possible combinations of χ^2 s and pick the one which is minimum as the χ^2 of the event. The combinations are done based on the two b -jet pairs and the possible solutions of $p_{z\nu}$. Since the χ^2 is constructed based on the signal, the χ^2 for the signal is expected to be very small compared to the background. We can see this feature in Fig.[3] for BP1 and BP6 where the signal is concentrated on small values of χ^2 and falls rapidly with χ^2 and for the background the distribution is very broad. Here as a signal we consider the $4b + \ell + \cancel{E}_T$ final state only through AAW mode and $t\bar{t}$ +jets as the background. Also the distributions are obtained after imposing the basic selection cuts which we will discuss in Sec.[3.2].

3.2 Signal-background analysis

In this section, we perform the signal-background analysis for the final state $4b + \ell + \cancel{E}_T$ at the LHC through the detector simulation. The signal considered so far is the AAW mode as given in Eq.[3.1]. There can be additional contributions to $4b + \ell + \cancel{E}_T$ from other EW processes as given below:

$$\begin{aligned}
 AAW &: pp \rightarrow H^\pm H \rightarrow (AW)(AA) \rightarrow 4b + \ell + \cancel{E}_T + X, \\
 AAZW &: pp \rightarrow H^\pm H \rightarrow (AW)(AZ) \rightarrow 4b + \ell + \cancel{E}_T + X, \\
 AAWW &: pp \rightarrow H^+ H^- \rightarrow (AW)(AW) \rightarrow 4b + \ell + \cancel{E}_T + X
 \end{aligned} \tag{3.13}$$

however, their contributions at the parton or generator level is subdominant compared to the AAW mode. Here X can be any jets (including b -jets) and/or leptons. Note that in the AAZW process we allow all possible decay modes of Z boson. Since the QCD corrections are only through the initial states and it would be same for the charged current and neutral current, the same k -factor of 1.35 can be imposed to all the EW processes. The cross

sections at the parton level for 13 TeV LHC are given by

$$\begin{aligned}
\sigma_{AAAW} &= \sigma(pp \rightarrow H^\pm H) BR(H^\pm \rightarrow AW) BR(H \rightarrow AA) BR(A \rightarrow b\bar{b})^2 \\
&\quad BR(W \rightarrow \ell\nu) [3 - 2BR(A \rightarrow b\bar{b})], \\
\sigma_{AAZW} &= \sigma(pp \rightarrow H^\pm H) BR(H^\pm \rightarrow AW) BR(H \rightarrow AZ) BR(A \rightarrow b\bar{b})^2 \\
&\quad BR(W \rightarrow \ell\nu), \\
\sigma_{AAWW} &= \sigma(pp \rightarrow H^\pm H^\pm) BR(H^\pm \rightarrow AW)^2 BR(A \rightarrow b\bar{b})^2 BR(W \rightarrow \ell\nu) \\
&\quad [2 - BR(W \rightarrow \ell\nu)].
\end{aligned} \tag{3.14}$$

The cross sections are based on at least four b -quarks and at least one lepton. The leptonic decay of W boson includes τ as well. For Monte Carlo event generation, the type I 2HDM model is first implemented in `FeynRules-2.3` [91]. Then the event generation for signal and background are done using `MadGraph5_aMC@NLO` [92] with `NNPDF31_lo_as_118` parton distribution functions set [93]. We used `PYTHIA-8.2` [94] for parton showering and hadronization. For detector simulation we used `Delphes-3.4.2` [95]. We use anti-kt algorithm [96] with radius parameter $R = 0.4$ and $p_T(j) > 20$ GeV for jet reconstruction. We also followed the default b -jet (mis-)tagging efficiencies as given in the `Delphes` CMS card based on Ref.[63]. After the generation of signal and background events, we impose the following basic selection cuts:

1. We select events with at least four b -jets and at least one lepton (e, μ).
2. The b -jets and lepton(s) are required to satisfy the criteria

$$p_T^b > 20 \text{ GeV}, \quad p_T^\ell > 10 \text{ GeV}, \quad |\eta^{b,\ell}| < 2.5.$$

3. We impose a nominal cut on the missing transverse energy (MET): $E_T > 10$ GeV.

The total signal cross sections for the final state $4b + \ell + E_T$ after imposing the basic selection cuts are shown in Fig.[4]. There is a spread in the cross section if we compare with Fig.[1] because of the contributions coming from the subdominant channels which depend on other model parameters like M^2 through $H \rightarrow AA$ decay and $s_{\beta-\alpha}$ through $H^\pm H$ production. We also see that the mass splitting between H^\pm and H is restricted due to the constraints from the EWPOs. The tagging of four b -jets at the detector reduces the cross sections of the signal to few fb whereas the cross section of the background after the basic selection is 772.2 fb which is still significantly higher than the proposed signal.

Therefore we resort to additional selection cuts as given below:

1. We impose a strong selection cut on χ^2 , which is

$$\chi^2 < 1 \tag{3.15}$$

to eliminate the background significantly. Even though we have additional sources of signal via EW processes Eq.[3.13] to the $4b + \ell + E_T$ final state. We impose the same χ^2 as given in Eq.[3.6], since their contribution at the generator level is subdominant.

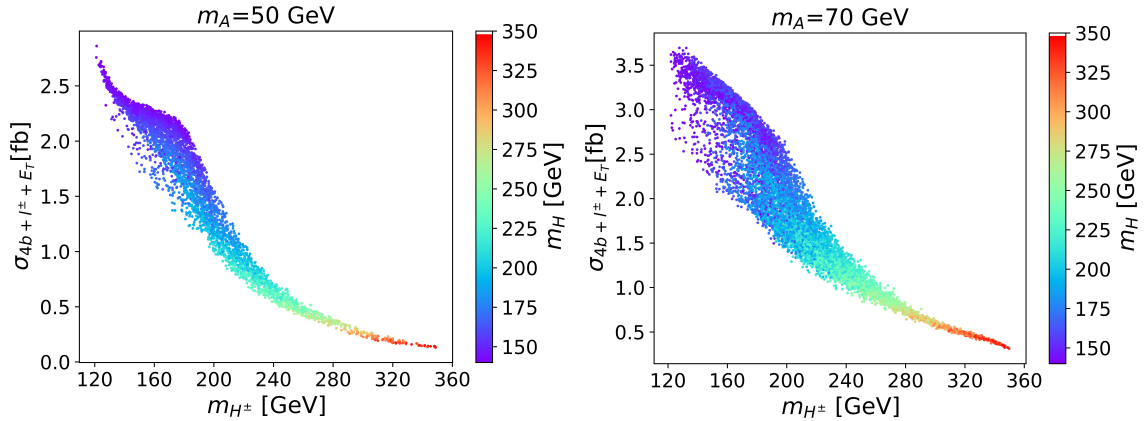


Figure 4. Total signal cross sections at the detector level with basic selection cuts. Left: $m_A = 50$ GeV and Right: $m_A = 70$ GeV.

2. After that, we require that the two pairs of b -jets which are obtained by the pairing algorithm should satisfy the asymmetry cut [90]

$$\alpha = \frac{|m_1 - m_2|}{m_1 + m_2} < 0.1 \quad (3.16)$$

where m_1 and m_2 are the invariant masses of the two b -jet pairs. The asymmetry cut ensures that the two b -jet pairs are from identical sources (AA pair in our signal). The asymmetry cut suits best to the dominant AAW mode, however just like the χ^2 cut we apply the same asymmetry cut to the other signals as they contribute subdominantly at the generator level.

3. Finally we impose the η separation of the b -jet pairs to satisfy

$$\Delta\eta = |\eta_1 - \eta_2| < 1.1 \quad (3.17)$$

to reduce the background contributions via t -channel process [90]. Here η_1 and η_2 are defined as

$$\eta_1 = \frac{\eta_a + \eta_b}{2}, \quad \eta_2 = \frac{\eta_c + \eta_d}{2} \quad (3.18)$$

where (a, b) and (c, d) are the two b -jet pairs obtained by the pairing algorithm.

We can now estimate discovery prospects of the $4b + \ell + \cancel{E}_T$ signal at the 13 TeV LHC for 3000 fb^{-1} luminosity by using the significance estimator given by [97]

$$S = \sqrt{2 \left[(N_s + N_b) \log \left(1 + \frac{N_s}{N_b} \right) - N_s \right]} \quad (3.19)$$

where N_s and N_b are the number of signal and background events obtained after imposing all the selection cuts. To see the discovery reach of the signal we use the BPs as given in Table. [2]. The χ^2 method would hold as long as the W boson is produced on-shell. Hence

| Cut Flow | Signals | Modes | Parton Level | Basic Cut | $\chi^2 < 1$ | $\alpha < 0.1$ | $\Delta\eta < 1.1$ | Significance |
|----------------|---------|-------|--------------|-----------|--------------|----------------|--------------------|--------------|
| $m_A = 50$ GeV | BP1 | AAW | 125.69 | 0.504 | 0.239 | 0.164 | 0.132 | 13.16 |
| | | AAAW | 37.59 | 1.174 | 0.143 | 0.081 | 0.069 | |
| | | AAZW | 5.01 | 0.048 | 0.005 | 0.003 | 0.002 | |
| | | AAWW | 35.26 | 0.317 | 0.043 | 0.027 | 0.024 | |
| | | BG | 458000 | 772.2 | 5.04 | 1.28 | 0.82 | |
| | BP2 | AAW | 57.62 | 0.440 | 0.268 | 0.177 | 0.144 | 5.91 |
| | | AAAW | 1.36 | 0.074 | 0.013 | 0.005 | 0.004 | |
| | | AAZW | 14.53 | 0.303 | 0.051 | 0.025 | 0.021 | |
| | | AAWW | 13.54 | 0.221 | 0.055 | 0.033 | 0.027 | |
| | | BG | 458000 | 772.2 | 28.85 | 6.41 | 3.21 | |
| | BP3 | AAW | 30.72 | 0.298 | 0.181 | 0.122 | 0.096 | 3.13 |
| | | AAAW | 1.13 | 0.077 | 0.012 | 0.004 | 0.003 | |
| | | AAZW | 5.45 | 0.155 | 0.029 | 0.014 | 0.011 | |
| | | AAWW | 6.51 | 0.115 | 0.032 | 0.019 | 0.013 | |
| | | BG | 458000 | 772.2 | 58.62 | 9.39 | 4.58 | |
| $m_A = 70$ GeV | BP4 | AAW | 72.73 | 0.665 | 0.372 | 0.230 | 0.194 | 11.20 |
| | | AAAW | 33.18 | 1.306 | 0.282 | 0.137 | 0.117 | |
| | | AAZW | 0.002 | – | – | – | – | |
| | | AAWW | 25.00 | 0.379 | 0.078 | 0.042 | 0.035 | |
| | | BG | 458000 | 772.2 | 18.23 | 4.40 | 2.75 | |
| | BP5 | AAW | 38.84 | 0.592 | 0.321 | 0.213 | 0.169 | 4.93 |
| | | AAAW | 5.20 | 0.363 | 0.077 | 0.039 | 0.032 | |
| | | AAZW | 8.13 | 0.244 | 0.050 | 0.027 | 0.022 | |
| | | AAWW | 10.79 | 0.284 | 0.070 | 0.042 | 0.033 | |
| | | BG | 458000 | 772.2 | 43.05 | 13.97 | 8.02 | |
| | BP6 | AAW | 20.20 | 0.394 | 0.244 | 0.161 | 0.127 | 2.92 |
| | | AAAW | 1.32 | 0.139 | 0.032 | 0.014 | 0.011 | |
| | | AAZW | 3.75 | 0.165 | 0.044 | 0.022 | 0.017 | |
| | | AAWW | 4.79 | 0.164 | 0.056 | 0.033 | 0.026 | |
| | | BG | 458000 | 772.2 | 98.93 | 21.76 | 11.45 | |

Table 4. The cut-flow table of the cross sections (in units of fb) for the signal and background with $m_A = 50$ GeV and 70 GeV at the 13 TeV LHC. Here "–" implies that the cross sections are insignificant. The significances are estimated for 3000 fb^{-1} luminosity.

in our analysis for the computation of significance, we only consider the BPs for which $H^\pm \rightarrow AW$ is on-shell. In Table. [4], the cross sections for the signal (dominant as well as subdominant contributions) and background are given with the selection cuts imposed sequentially. The basic cut depends only on the tagging efficiencies of $4b$ -jets. Since the *AAAW* mode has an additional A compared to the *AAW* mode, it allows for the possibility

of additional b -jets. As a result, the $4b$ tagging efficiency is higher for the $AAAW$ mode, leading to its dominance over the AAW mode at the basic cut for some BPs, despite lower cross sections at the parton level. The χ^2 discriminator is based on the AAW mode, and therefore, as we move from the basic cut to the χ^2 cut, the AAW mode dominates over the $AAAW$ mode⁴. Comparing the signal and the background, we can clearly see that the χ^2 cut kills the background significantly. Thus from our analysis with six BPs selected over a wide range of masses, we demonstrate that the signal significance greater than 3σ can be achieved.

For our analysis we considered only two scenarios for the pseudoscalar mass: 50 GeV and 70 GeV. The former scenario is chosen to explore the situation when $h \rightarrow AA$ is possible, while the second scenario is chosen where $h \rightarrow AA$ is not allowed. Additionally, one could also consider scenarios with a slightly higher mass for A , such as $m_A = 110$ GeV and the remaining BSM Higgs bosons heavier than A . In that case, $\text{BR}(A \rightarrow b\bar{b})$ is approximately 70%, and we expect good results for such scenarios as well. However, it should be noted that the EW production cross section of the AAW mode will decrease as the cumulative mass of H^\pm and A increases. Consequently, the significance will be relatively low for higher masses of H^\pm . For $m_A > m_{h,H,H^\pm}$, the bosonic decay modes of A , such as $A \rightarrow hZ^{(*)}/HZ^{(*)}/H^\pm W^{(*)}$, will become accessible and may dominate over the $A \rightarrow b\bar{b}$ mode in the fermiophobic limit (large t_β). Thus, in the context of the $4b + \ell + \cancel{E}_T$ final state in type I 2HDM with standard mass hierarchy, choosing the pseudoscalar as the lightest of all the Higgs bosons would be appropriate.

Before we conclude, we would like to point out how the χ^2 discriminator can be applied to real data at the LHC as a selection criteria in the context of BSM Higgs boson searches. The experimentalists should examine the normalized χ^2 distributions using real data. When the correct hypothesis (masses of A and H^\pm) is used as input to the χ^2 discriminator, the resulting χ^2 distribution will exhibit a declining pattern with respect to χ^2 , similar to the signals shown in Fig.[3]. Concurrently, experimentalists should vary (or make a proper scan) the masses of A and H^\pm to determine the values that yield the steepest decline in the χ^2 distribution. These identified masses of A and H^\pm represent the correct masses of A and H^\pm that exist within the signal. Not only that, for the correctly identified masses which shows the steepest decline in the χ^2 distribution, the χ^2 cut would give very high discovery significance.

4 Conclusions

The EW multi-Higgs production in various BSM frameworks can be dominant compared to the QCD induced processes due to the non-standard couplings of the additional Higgs bosons. In type I 2HDM, for a large region of parameter space, all the additional Higgses exhibit fermiophobic behaviour and hence, the EW processes are dominant. Not only that, the EW processes can also be $q\bar{q}'$ induced, which results into charged final states like $pp \rightarrow H^\pm A \rightarrow AAW$ and therefore $4b + \ell + \cancel{E}_T$ final state for light pseudoscalar at

⁴While the $AAAW$ mode can give rise to the $6b + \ell + \cancel{E}_T$ final state, tagging $6b$ -jets, especially for background events, is extremely challenging. Hence, we refrain from pursuing studies in this direction.

the LHC which cannot be achieved through QCD processes. Thus, alongside the QCD induced processes, systematic analysis based on the EW processes should be done both phenomenologically and experimentally.

In this work we studied the $4b + \ell + \cancel{E}_T$ final state at 13 TeV LHC with a luminosity of 3000 fb^{-1} . However, the signal is obscured by large $t\bar{t}$ +jets background. Hence strong selection cuts are to be imposed to kill the background without much affecting the signal. The dominant contribution to the $4b + \ell + \cancel{E}_T$ final state at the generator level comes through the AAW mode, we use this signal topology and the BSM Higgs mass informations like the masses of A and H^\pm (signal hypothesis) to construct the χ^2 variable. We briefly summarize the χ^2 method in the following steps:

1. First we imposed a b -jet pairing algorithm to make two b -jet pairs out of the four leading b -jets.
2. Assuming that the MET corresponds to only one neutrino from the leptonic decay of the W boson in the AAW mode, we estimated the $p_{z\nu}$ component of neutrino momentum.
3. We did the truth reconstruction of the BSM Higgs bosons (A and H^\pm) involved in the AAW mode to obtain the mass resolutions. These mass resolutions are used as inputs to the χ^2 .
4. Finally, we make all possible combinations of χ^2 s and pick the one which is minimum as the χ^2 of the event.

The χ^2 serves as a powerful tool to discriminate the signal from the background. We showed that the χ^2 distribution for the AAW signal falls very sharply with χ^2 whereas the background distribution is very broad. Our formalism for χ^2 is appropriate only for on-shell W boson and therefore scenarios restricted to on-shell $H^\pm \rightarrow AW$ processes and also for W boson decaying to the leptonic state with one neutrino. Since the contribution of more than one neutrino and electron/muon via taonic decay of W boson is negligibly small, we can safely apply the χ^2 method even if the signal is generated with $W \rightarrow \ell\nu$ and ℓ includes τ lepton. We impose $\chi^2 < 1$ and other selection cuts like asymmetry cut and di-jet η separation cut to effectively reduce the background. To study the discovery prospects of $4b + \ell + \cancel{E}_T$ final state at the LHC, we considered the subdominant EW processes along with the primary AAW mode and obtained the discovery significance greater than 3σ over a wide range of parameter space.

Acknowledgments

The authors thank Ravindra K. Verma for some useful discussions. The authors would also like to thank Stefano Moretti and Jeonghyeon Song for careful reading and useful comments. The work is supported by the National Research Foundation of Korea, Grant No. NRF-2022R1A2C1007583.

References

- [1] ATLAS collaboration, *Observation of a new particle in the search for the standard model higgs boson with the atlas detector at the lhc*, [Phys. Lett. B](#) **716** (2012) 1 [[1207.7214](#)].
- [2] CMS collaboration, *Observation of a New Boson at a Mass of 125 GeV with the CMS Experiment at the LHC*, [Phys. Lett. B](#) **716** (2012) 30 [[1207.7235](#)].
- [3] ATLAS collaboration, *Measurements of higgs boson production and couplings in diboson final states with the atlas detector at the lhc*, [Phys. Lett. B](#) **726** (2013) 88 [[1307.1427](#)].
- [4] CMS collaboration, *Observation of a New Boson with Mass Near 125 GeV in pp Collisions at $\sqrt{s} = 7$ and 8 TeV*, [JHEP](#) **06** (2013) 081 [[1303.4571](#)].
- [5] G.C. Branco, P.M. Ferreira, L. Lavoura, M.N. Rebelo, M. Sher and J.P. Silva, *Theory and phenomenology of two-Higgs-doublet models*, [Phys. Rept.](#) **516** (2012) 1 [[1106.0034](#)].
- [6] J.F. Gunion and H.E. Haber, *The CP conserving two Higgs doublet model: The Approach to the decoupling limit*, [Phys. Rev. D](#) **67** (2003) 075019 [[hep-ph/0207010](#)].
- [7] J.F. Gunion, H.E. Haber, G.L. Kane and S. Dawson, *The Higgs Hunter's Guide*, vol. 80 (2000).
- [8] S. Davidson and H.E. Haber, *Basis-independent methods for the two-Higgs-doublet model*, [Phys. Rev. D](#) **72** (2005) 035004 [[hep-ph/0504050](#)].
- [9] S.L. Glashow and S. Weinberg, *Natural Conservation Laws for Neutral Currents*, [Phys. Rev. D](#) **15** (1977) 1958.
- [10] E.A. Paschos, *Diagonal Neutral Currents*, [Phys. Rev. D](#) **15** (1977) 1966.
- [11] A. Arhrib, R. Benbrik, R.B. Guedes and R. Santos, *Search for a light fermiophobic Higgs boson produced via gluon fusion at Hadron Colliders*, [Phys. Rev. D](#) **78** (2008) 075002 [[0805.1603](#)].
- [12] B. Hespel, D. Lopez-Val and E. Vryonidou, *Higgs pair production via gluon fusion in the Two-Higgs-Doublet Model*, [JHEP](#) **09** (2014) 124 [[1407.0281](#)].
- [13] D. Dicus, T. Stelzer, Z. Sullivan and S. Willenbrock, *Higgs boson production in association with bottom quarks at next-to-leading order*, [Phys. Rev. D](#) **59** (1999) 094016 [[hep-ph/9811492](#)].
- [14] C. Balazs, H.-J. He and C.P. Yuan, *QCD corrections to scalar production via heavy quark fusion at hadron colliders*, [Phys. Rev. D](#) **60** (1999) 114001 [[hep-ph/9812263](#)].
- [15] R.V. Harlander and W.B. Kilgore, *Higgs boson production in bottom quark fusion at next-to-next-to leading order*, [Phys. Rev. D](#) **68** (2003) 013001 [[hep-ph/0304035](#)].
- [16] C. Duhr, F. Dulat, V. Hirschi and B. Mistlberger, *Higgs production in bottom quark fusion: matching the 4- and 5-flavour schemes to third order in the strong coupling*, [JHEP](#) **08** (2020) 017 [[2004.04752](#)].
- [17] CMS collaboration, *Search for resonant pair production of Higgs bosons decaying to bottom quark-antiquark pairs in proton-proton collisions at 13 TeV*, [JHEP](#) **08** (2018) 152 [[1806.03548](#)].
- [18] ATLAS collaboration, *Search for new phenomena in events with at least three photons collected in pp collisions at $\sqrt{s} = 8$ TeV with the ATLAS detector*, [Eur. Phys. J. C](#) **76** (2016) 210 [[1509.05051](#)].

- [19] CMS collaboration, *Search for MSSM Higgs bosons decaying to $\mu + \mu -$ in proton-proton collisions at $s=13\text{TeV}$* , [Phys. Lett. B **798** \(2019\) 134992 \[1907.03152\]](#).
- [20] ATLAS collaboration, *Search for scalar resonances decaying into $\mu^+\mu^-$ in events with and without b -tagged jets produced in proton-proton collisions at $\sqrt{s} = 13$ TeV with the ATLAS detector*, [JHEP **07** \(2019\) 117 \[1901.08144\]](#).
- [21] CMS collaboration, *Search for beyond the standard model Higgs bosons decaying into a $b\bar{b}$ pair in pp collisions at $\sqrt{s} = 13$ TeV*, [JHEP **08** \(2018\) 113 \[1805.12191\]](#).
- [22] ATLAS collaboration, *Search for heavy Higgs bosons decaying into two tau leptons with the ATLAS detector using pp collisions at $\sqrt{s} = 13$ TeV*, [Phys. Rev. Lett. **125** \(2020\) 051801 \[2002.12223\]](#).
- [23] CMS collaboration, *Search for a low-mass $\tau^+\tau^-$ resonance in association with a bottom quark in proton-proton collisions at $\sqrt{s} = 13$ TeV*, [JHEP **05** \(2019\) 210 \[1903.10228\]](#).
- [24] M. Flechl, R. Klees, M. Kramer, M. Spira and M. Ubiali, *Improved cross-section predictions for heavy charged Higgs boson production at the LHC*, [Phys. Rev. D **91** \(2015\) 075015 \[1409.5615\]](#).
- [25] C. Degrande, M. Ubiali, M. Wiesemann and M. Zaro, *Heavy charged Higgs boson production at the LHC*, [JHEP **10** \(2015\) 145 \[1507.02549\]](#).
- [26] CMS collaboration, *Search for charged Higgs bosons in the $H^\pm \rightarrow \tau^\pm\nu_\tau$ decay channel in proton-proton collisions at $\sqrt{s} = 13$ TeV*, [JHEP **07** \(2019\) 142 \[1903.04560\]](#).
- [27] ATLAS collaboration, *Search for charged Higgs bosons decaying into a top quark and a bottom quark at $\sqrt{s} = 13$ TeV with the ATLAS detector*, [JHEP **06** \(2021\) 145 \[2102.10076\]](#).
- [28] A.G. Akeroyd, *Fermiophobic Higgs bosons at the Tevatron*, [Phys. Lett. B **368** \(1996\) 89 \[hep-ph/9511347\]](#).
- [29] A.G. Akeroyd, *Fermiophobic and other nonminimal neutral Higgs bosons at the LHC*, [J. Phys. G **24** \(1998\) 1983 \[hep-ph/9803324\]](#).
- [30] A. Arhrib, R. Benbrik and S. Moretti, *Bosonic Decays of Charged Higgs Bosons in a 2HDM Type-I*, [Eur. Phys. J. C **77** \(2017\) 621 \[1607.02402\]](#).
- [31] R. Enberg, W. Klemm, S. Moretti and S. Munir, *Electroweak production of multiple (pseudo)scalars in the 2HDM*, [Eur. Phys. J. C **79** \(2019\) 512 \[1812.01147\]](#).
- [32] F. Kling, S. Su and W. Su, *2HDM Neutral Scalars under the LHC*, [JHEP **06** \(2020\) 163 \[2004.04172\]](#).
- [33] Y. Wang, A. Arhrib, R. Benbrik, M. Krab, B. Manaut, S. Moretti et al., *Analysis of $W + 4\gamma$ in the 2HDM Type-I at the LHC*, [JHEP **12** \(2021\) 021 \[2107.01451\]](#).
- [34] H. Bahl, T. Stefaniak and J. Wittbrodt, *The forgotten channels: charged Higgs boson decays to a W and a non-SM-like Higgs boson*, [JHEP **06** \(2021\) 183 \[2103.07484\]](#).
- [35] A. Arhrib, R. Benbrik, M. Krab, B. Manaut, S. Moretti, Y. Wang et al., *New discovery modes for a light charged Higgs boson at the LHC*, [JHEP **10** \(2021\) 073 \[2106.13656\]](#).
- [36] T. Mondal and P. Sanyal, *Same sign trilepton as signature of charged Higgs in two Higgs doublet model*, [JHEP **05** \(2022\) 040 \[2109.05682\]](#).
- [37] J. Kim, S. Lee, J. Song and P. Sanyal, *Fermiophobic light Higgs boson in the type-I two-Higgs-doublet model*, [Phys. Lett. B **834** \(2022\) 137406 \[2207.05104\]](#).

- [38] J. Kim, S. Lee, P. Sanyal, J. Song and D. Wang, $\tau\nu\gamma\gamma$ and *[inline-graphic not available: see fulltext]* to probe the fermiophobic Higgs boson with high cutoff scales, [JHEP 04 \(2023\) 083](#) [[2302.05467](#)].
- [39] S.K. Kang, J. Kim, S. Lee and J. Song, *Disentangling the high- and low-cutoff scales via the trilinear Higgs couplings in the type-I two-Higgs-doublet model*, [Phys. Rev. D 107 \(2023\) 015025](#) [[2210.00020](#)].
- [40] Z. Li, A. Arhrib, R. Benbrik, M. Krab, B. Manaut, S. Moretti et al., *Discovering a light charged Higgs boson via $W^{\pm*} + 4b$ final states at the LHC*, [2305.05788](#).
- [41] A. Arhrib, R. Benbrik, R. Enberg, W. Klemm, S. Moretti and S. Munir, *Identifying a light charged Higgs boson at the LHC Run II*, [Phys. Lett. B 774 \(2017\) 591](#) [[1706.01964](#)].
- [42] D. Bhatia, N. Desai and S. Dwivedi, *Discovery prospects of a light charged Higgs near the fermiophobic region of Type-I 2HDM*, [JHEP 06 \(2023\) 100](#) [[2212.14363](#)].
- [43] CMS collaboration, *Search for pair production of excited top quarks in the lepton + jets final state*, [Phys. Lett. B 778 \(2018\) 349](#) [[1711.10949](#)].
- [44] T. Mondal, S. Moretti, S. Munir and P. Sanyal, *Electroweak multi-Higgs production: A smoking gun for the Type-I 2HDM*, [2304.07719](#).
- [45] CMS collaboration, *Evidence for Higgs boson decay to a pair of muons*, [JHEP 01 \(2021\) 148](#) [[2009.04363](#)].
- [46] I.L. Buchbinder, E.A. Ivanov, B.S. Merzlikin and K.V. Stepanyantz, *The renormalization structure of 6D, $\mathcal{N} = (1, 0)$ supersymmetric higher-derivative gauge theory*, [Nucl. Phys. B 961 \(2020\) 115249](#) [[2007.02843](#)].
- [47] ATLAS collaboration, *Measurements of higgs bosons decaying to bottom quarks from vector boson fusion production with the atlas experiment at $\sqrt{s} = 13$ TeV*, [Eur. Phys. J. C 81 \(2021\) 537](#) [[2011.08280](#)].
- [48] CMS collaboration, *Inclusive search for highly boosted higgs bosons decaying to bottom quark-antiquark pairs in proton-proton collisions at $\sqrt{s} = 13$ tev*, [JHEP 12 \(2020\) 085](#) [[2006.13251](#)].
- [49] ATLAS collaboration, *Study of higgs boson production with large transverse momentum using the $h \rightarrow b\bar{b}$ decay with the atlas detector*, .
- [50] CMS collaboration, *Measurement of the inclusive and differential higgs boson production cross sections in the decay mode to a pair of τ leptons in pp collisions at $\sqrt{s} = 13$ tev*, [Phys. Rev. Lett. 128 \(2022\) 081805](#) [[2107.11486](#)].
- [51] ATLAS collaboration, *Measurement of the higgs boson decaying to b-quarks produced in association with a top-quark pair in pp collisions at $\sqrt{s} = 13$ tev with the atlas detector*, .
- [52] ATLAS collaboration, *Measurements of gluon fusion and vector-boson-fusion production of the higgs boson in $h \rightarrow ww^* \rightarrow e\nu\mu\nu$ decays using pp collisions at $\sqrt{s} = 13$ tev with the atlas detector*, .
- [53] CMS collaboration, *Measurements of production cross sections of the higgs boson in the four-lepton final state in proton-proton collisions at $\sqrt{s} = 13$ TeV*, [Eur. Phys. J. C 81 \(2021\) 488](#) [[2103.04956](#)].
- [54] ATLAS collaboration, *Measurements of the higgs boson inclusive and differential fiducial*

- cross sections in the 4ℓ decay channel at $\sqrt{s} = 13$ tev, [Eur. Phys. J. C **80** \(2020\) 942 \[2004.03969\]](#).
- [55] ATLAS collaboration, *Higgs boson production cross-section measurements and their eft interpretation in the 4ℓ decay channel at $\sqrt{s} = 13$ tev with the atlas detector*, [Eur. Phys. J. C **80** \(2020\) 957 \[2004.03447\]](#).
- [56] ATLAS collaboration, *A search for the dimuon decay of the Standard Model Higgs boson with the ATLAS detector*, [Phys. Lett. B **812** \(2021\) 135980 \[2007.07830\]](#).
- [57] ATLAS collaboration, *Direct constraint on the higgs-charm coupling from a search for higgs boson decays into charm quarks with the atlas detector*, [Eur. Phys. J. C **82** \(2022\) 717 \[2201.11428\]](#).
- [58] P. Basler, P.M. Ferreira, M. Mühlleitner and R. Santos, *High scale impact in alignment and decoupling in two-Higgs doublet models*, [Phys. Rev. D **97** \(2018\) 095024 \[1710.10410\]](#).
- [59] V. Branchina, F. Contino and P.M. Ferreira, *Electroweak vacuum lifetime in two Higgs doublet models*, [JHEP **11** \(2018\) 107 \[1807.10802\]](#).
- [60] J. Alwall et al., *Comparative study of various algorithms for the merging of parton showers and matrix elements in hadronic collisions*, [Eur. Phys. J. C **53** \(2008\) 473 \[0706.2569\]](#).
- [61] S. Hoeche, F. Krauss, N. Lavesson, L. Lonnblad, M. Mangano, A. Schallicke et al., *Matching parton showers and matrix elements*, in [HERA and the LHC: A Workshop on the Implications of HERA for LHC Physics: CERN - DESY Workshop 2004/2005 \(Midterm Meeting, CERN, 11-13 October 2004; Final Meeting, DESY, 17-21 January 2005\)](#), pp. 288–289, 2005, DOI [[hep-ph/0602031](#)].
- [62] M. Czakon and A. Mitov, *Top++: A Program for the Calculation of the Top-Pair Cross-Section at Hadron Colliders*, [Comput. Phys. Commun. **185** \(2014\) 2930 \[1112.5675\]](#).
- [63] CMS collaboration, *Identification of b-Quark Jets with the CMS Experiment*, [JINST **8** \(2013\) P04013 \[1211.4462\]](#).
- [64] A. Hammad, M. Park, R. Ramos and P. Saha, *Exploration of Parameter Spaces Assisted by Machine Learning*, [2207.09959](#).
- [65] S. Chang, S.K. Kang, J.-P. Lee and J. Song, *Higgs potential and hidden light Higgs scenario in two Higgs doublet models*, [Phys. Rev. D **92** \(2015\) 075023 \[1507.03618\]](#).
- [66] N.G. Deshpande and E. Ma, *Pattern of symmetry breaking with two higgs doublets*, [Phys. Rev. D **18** \(1978\) 2574](#).
- [67] S. Kanemura, T. Kubota and E. Takasugi, *Lee-Quigg-Thacker bounds for Higgs boson masses in a two doublet model*, [Phys. Lett. B **313** \(1993\) 155 \[hep-ph/9303263\]](#).
- [68] A.G. Akeroyd, A. Arhrib and E.-M. Naimi, *Note on tree level unitarity in the general two Higgs doublet model*, [Phys. Lett. B **490** \(2000\) 119 \[hep-ph/0006035\]](#).
- [69] D. Eriksson, J. Rathsman and O. Stal, *2HDMC: Two-Higgs-Doublet Model Calculator Physics and Manual*, [Comput. Phys. Commun. **181** \(2010\) 189 \[0902.0851\]](#).
- [70] P.D. Group, R.L. Workman, V.D. Burkert, V. Crede, E. Klempt, U. Thoma et al., *Review of Particle Physics*, [Progress of Theoretical and Experimental Physics **2022** \(2022\) \[https://academic.oup.com/ptep/article-pdf/2022/8/083C01/49175539/ptac097.pdf\]](#).
- [71] W. Grimus, L. Lavoura, O.M. Ogreid and P. Osland, *A Precision constraint on multi-Higgs-doublet models*, [J. Phys. G **35** \(2008\) 075001 \[0711.4022\]](#).

- [72] W. Grimus, L. Lavoura, O.M. Ogreid and P. Osland, *The Oblique parameters in multi-Higgs-doublet models*, [Nucl. Phys. B](#) **801** (2008) 81 [0802.4353].
- [73] F. Mahmoudi, *SuperIso v2.3: A Program for calculating flavor physics observables in Supersymmetry*, [Comput. Phys. Commun.](#) **180** (2009) 1579 [0808.3144].
- [74] HFLAV collaboration, *Averages of b-hadron, c-hadron, and τ -lepton properties as of summer 2016*, [Eur. Phys. J. C](#) **77** (2017) 895 [1612.07233].
- [75] M. Misiak and M. Steinhauser, *Weak radiative decays of the B meson and bounds on M_{H^\pm} in the Two-Higgs-Doublet Model*, [Eur. Phys. J. C](#) **77** (2017) 201 [1702.04571].
- [76] P. Sanyal, *Limits on the charged higgs parameters in the two higgs doublet model using cms $\sqrt{s} = 13$ tev results*, [Eur. Phys. J. C](#) **79** (2019) 913 [1906.02520].
- [77] P. Bechtle, D. Dercks, S. Heinemeyer, T. Klingl, T. Stefaniak, G. Weiglein et al., *HiggsBounds-5: Testing Higgs Sectors in the LHC 13 TeV Era*, [Eur. Phys. J. C](#) **80** (2020) 1211 [2006.06007].
- [78] P. Bechtle, S. Heinemeyer, T. Klingl, T. Stefaniak, G. Weiglein and J. Wittbrodt, *HiggsSignals-2: Probing new physics with precision Higgs measurements in the LHC 13 TeV era*, [Eur. Phys. J. C](#) **81** (2021) 145 [2012.09197].
- [79] ATLAS collaboration, *Search for the Higgs boson produced in association with a vector boson and decaying into two spin-zero particles in the $H \rightarrow aa \rightarrow 4b$ channel in pp collisions at $\sqrt{s} = 13$ TeV with the ATLAS detector*, [JHEP](#) **10** (2018) 031 [1806.07355].
- [80] CMS collaboration, *Search for an exotic decay of the Higgs boson to a pair of light pseudoscalars in the final state with two b quarks and two τ leptons in proton-proton collisions at $\sqrt{s} = 13$ TeV*, [Phys. Lett. B](#) **785** (2018) 462 [1805.10191].
- [81] ATLAS collaboration, *Search for Higgs boson decays into a pair of light bosons in the $b\bar{b}\mu\mu$ final state in pp collision at $\sqrt{s} = 13$ TeV with the ATLAS detector*, [Phys. Lett. B](#) **790** (2019) 1 [1807.00539].
- [82] CMS collaboration, *Search for light bosons in decays of the 125 GeV Higgs boson in proton-proton collisions at $\sqrt{s} = 8$ TeV*, [JHEP](#) **10** (2017) 076 [1701.02032].
- [83] CMS collaboration, *Search for an exotic decay of the Higgs boson to a pair of light pseudoscalars in the final state with two muons and two b quarks in pp collisions at 13 TeV*, [Phys. Lett. B](#) **795** (2019) 398 [1812.06359].
- [84] CMS collaboration, *Search for an exotic decay of the Higgs boson to a pair of light pseudoscalars in the final state of two muons and two τ leptons in proton-proton collisions at $\sqrt{s} = 13$ TeV*, [JHEP](#) **11** (2018) 018 [1805.04865].
- [85] CMS collaboration, *A portrait of the Higgs boson by the CMS experiment ten years after the discovery*, [Nature](#) **607** (2022) 60 [2207.00043].
- [86] CMS collaboration, *Measurements of the Higgs boson width and anomalous HVV couplings from on-shell and off-shell production in the four-lepton final state*, [Phys. Rev. D](#) **99** (2019) 112003 [1901.00174].
- [87] CMS collaboration, *Measurement of the Higgs boson width and evidence of its off-shell contributions to ZZ production*, [Nature Phys.](#) **18** (2022) 1329 [2202.06923].
- [88] ATLAS collaboration, *Evidence of off-shell Higgs boson production from ZZ leptonic decay channels and constraints on its total width with the ATLAS detector*, [2304.01532](#).

- [89] CMS collaboration, *Search for pair-produced resonances decaying to quark pairs in proton-proton collisions at $\sqrt{s} = 13$ tev*, [Phys. Rev. D **98** \(2018\) 112014 \[1808.03124\]](#).
- [90] C. Collaborations, *Search for resonant and nonresonant production of pairs of dijet resonances in proton-proton collisions at $\sqrt{s} = 13$ tev*, Tech. Rep. [CMS-EXO-21-010, CERN-EP-2022-103, CMS-EXO-21-010-003](#), CERN, Geneva (2022).
- [91] A. Alloul, N.D. Christensen, C. Degrande, C. Duhr and B. Fuks, *FeynRules 2.0 - A complete toolbox for tree-level phenomenology*, [Comput. Phys. Commun. **185** \(2014\) 2250 \[1310.1921\]](#).
- [92] J. Alwall, M. Herquet, F. Maltoni, O. Mattelaer and T. Stelzer, *MadGraph 5 : Going Beyond*, [JHEP **06** \(2011\) 128 \[1106.0522\]](#).
- [93] NNPDF collaboration, *Parton distributions from high-precision collider data*, [Eur. Phys. J. C **77** \(2017\) 663 \[1706.00428\]](#).
- [94] T. Sjöstrand, S. Ask, J.R. Christiansen, R. Corke, N. Desai, P. Ilten et al., *An introduction to PYTHIA 8.2*, [Comput. Phys. Commun. **191** \(2015\) 159 \[1410.3012\]](#).
- [95] DELPHES 3 collaboration, *DELPHES 3, A modular framework for fast simulation of a generic collider experiment*, [JHEP **02** \(2014\) 057 \[1307.6346\]](#).
- [96] M. Cacciari, G.P. Salam and G. Soyez, *The anti- k_t jet clustering algorithm*, [JHEP **04** \(2008\) 063 \[0802.1189\]](#).
- [97] G. Cowan, K. Cranmer, E. Gross and O. Vitells, *Asymptotic formulae for likelihood-based tests of new physics*, [Eur. Phys. J. C **71** \(2011\) 1554 \[1007.1727\]](#).